Detecting serum and urine metabolic profile changes of CCl_4-liver fibrosis in rats at 12 weeks based on gas chromatography-mass spectrometry

JIARONG GAO[1], XIU-JUAN QIN[1], HUI JIANG[1], JIN-FENG CHEN[1], TING WANG[2], TING ZHANG[2], SHUANG-ZHI XU[2] and JUN-MEI SONG[2]

[1]Department of Pharmacy; [2]College of Pharmacy, The First Affiliated Hospital of Anhui University of Chinese Medicine, Hefei, Anhui 230031, P.R. China

Received September 11, 2015; Accepted October 18, 2016

DOI: 10.3892/etm.2017.4668

Abstract. Liver fibrosis is caused by liver injury induced by a number of chronic liver diseases, including schistosome infection, hepatitis infection, metabolic disease, alcoholism and cholestasis. The tissue damage occurring after injury or inflammation of the liver is a reversible lesion; however, liver fibrosis has become a worldwide problem and poses a threat to human health. The development of an effective drug for the prevention and treatment of liver fibrosis is ongoing and uses information from different occurrences of liver fibrosis. In the present study, carbon tetrachloride (CCl_4)-induced metabonomic changes in serum and urine at 12 weeks were analyzed using gas chromatography-mass spectrometry (GC/MS) to investigate potential biomarkers. Liver fibrosis was induced in rats by subcutaneous injections of CCl_4 twice a week for 12 consecutive weeks. Histopathological changes were used to assess the successful production of a CCl_4-induced liver fibrosis model. Serum and urine samples from the two groups were collected at 12 weeks. The metabolic profile changes were analyzed by GC/MS alongside principal component analysis and orthogonal projections to latent structures. Metabolic profile studies indicated that the clustering of the two groups could be separated and seven metabolites in serum and five metabolites in urine were identified. In serum, the metabolites identified included isoleucine, L-malic acid, α-copper, carnitine, hippuric acid, glutaric acid and glucose. In urine 2-hydroxy butyric acid, isoleucine, N-acetyl-β-alanine, cytidine and corticoid were identified. The present study demonstrated that the pathogenesis of liver fibrosis may be associated with the dysfunction of a number of metabolic pathways, including glucose, amino acid, P450, fatty acid, nucleic acid, water-electrolyte and glutathione biosynthesis. Assessing potential biomarkers may therefore provide novel targets and theories for the innovation of novel drugs to prevent and cure liver fibrosis.

Introduction

Liver fibrosis occurs as a wound-healing process following liver injury induced by chronic liver disease and is identified by an exorbitant accumulation of extracellular matrix (ECM), scar tissue or collagen (1). The deposition of ECM proteins substitute for functional tissues and disrupt the normal liver architecture, which in turn leads to pathophysiological damage (2). The primary causes of liver fibrosis include chronic high alcohol ingestion and infection with hepatitis B and C. Less common causes include viral infection, hemochromatosis, primary biliary cirrhosis, primary sclerosing cholangitis, helminth infection, autoimmune diseases and nonalcoholic steatohepatitis (3). Hepatic fibrosis is a vital stage that occurs during the development of chronic liver disease. Cirrhosis and hepatocellular carcinomas are of great concern worldwide due to the high morbidity and mortality rates associated with them (4). There are currently no effective therapies to treat liver cirrhosis; however, it has been suggested that the damage may be reversible if treated appropriately during the early, fibrotic stage of cirrhosis (5). Therefore, identifying an effective treatment for hepatic fibrosis is critical in order to decrease the chances of patients with hepatic fibrosis developing chronic liver disease.

Liver biopsy is the gold standard of diagnosis for different stages of fibrosis and inflammation. However, this technique

Correspondence to: Professor Jiarong Gao, Department of Pharmacy, The First Affiliated Hospital of Anhui University of Chinese Medicine, 117 Meishan Road, Hefei, Anhui 230031, P.R. China
E-mail: zyfygjr2006@163.com

Abbreviations: CCl_4, carbon tetrachloride; GC/MS, gas chromatography-mass spectrometry; PCA, principal component analysis; OPLS, orthogonal projections to latent structures; DA, discriminant analysis; ECM, extracellular matrix; H&E, hematoxylin and eosin; BSTFA, bis-(trimethylsilyl) trifluoroacetamide; SPSS, Statistic Package for Social Science; TIC, total ion current; VIP, variable importance projection; KEGG, Kyoto Encyclopedia of Genes and Genomes; TCA, triglycerides; acetyl-CoA, acetyl-coenzyme A; RAAS, renin-angiotensin-aldosterone system

Key words: hepatic fibrosis, carbon tetrachloride, serum, urine, metabonomics, gas chromatography-mass spectrometry

may cause complications including bleeding, pain, bile peritonitis, pneumothorax and mortality. Furthermore, there are problems due to the procedure being invasive and sampling errors occurring (6,7). Vessel imaging serves a crucial role in the diagnosis of hepatic fibrosis. Additionally, vessel imaging can help test for hepatic fibrosis in the early stages, making it useful for investigating the development of hepatic fibrosis (8). However, traditional imaging techniques widely used in clinical practice, including magnetic resonance elastography and conventional radiography, are ineffective at detecting mild to moderate hepatic fibrosis, particularly in obese patients (9,10). In recent years, technological developments have led to a novel, non-invasive method, protein fingerprinting of the extracellular matrix remodeling (11), which is being developed to diagnose hepatic fibrosis. The method includes biochemical and hematological tests and the assessment of serum biomarkers in connective tissue. However, it has no sensitive, specific or reproducible application methods to detect the early stages of fibrosis (11). Thus, it is important to investigate other treatment options and identify effective techniques for the early diagnosis of liver fibrosis. Liver fibrosis biomarkers and characterization of metabolic changes indicate that the onset of fibrosis occurs earlier than other diagnostic forms, including noninvasive diagnostics such as imaging diagnosis (12). This may provide an effective way to detect liver fibrosis early, enabling the administration of effective treatment and a clearer understanding of the molecular mechanisms.

Metabonomics is a comprehensive analytical technology used to study biological systems and is defined as 'the quantitative measurement of the dynamic multi-parametric responses of a living system to pathophysiological stimuli or genetic modification' (13). Metabonomics screens for metabolic biomarkers to detect related endogenous metabolites, toxicological and pharmacological effects, describe metabolic pathways, and explain the function of complex biological systems to distinguish disease states (14). A number of analytical platforms have been employed for metabonomic analysis, including liquid chromatography coupled with mass spectrometry, nuclear magnetic resonance, high-performance liquid chromatography/mass spectrometry and gas chromatography-mass spectrophotometry (GC/MS) (15). GC/MS is a major analytical tool for metabonomic studies used to analyze various types of samples including those from the serum, urine, cerebrospinal fluid and plasma. GC/MS produces results at a high resolution, reproducibility, sensitivity and accuracy while being simple and providing good separability (16). Multivariate statistical methods, Including principal component analysis (PCA) and orthogonal projections to latent structures (OPLS) are generally used to assess metabonomic data collected by GC/MS. PCA is an unsupervised mode recognition method that changes a range of correlated variables into a number of smaller uncorrelated variables called principal components. OPLS-discriminant analysis (OPLS-DA) is a method of discerning between two or more groups so that differences in variables may be identified. These methods provide classification of observations and a vast amount of information regarding the latent structures by regression during the modeling (17).

The present study investigated the main pharmacodynamics index, assessed changes to serum and urine metabolite group pathways that occur during liver fibrosis and identified potential biomarkers for liver fibrosis using GC/MS. The study aimed to examine the practicality of GC/MS in the study of metabonomics and provide novel targets for innovative drugs to treat liver fibrosis.

Materials and methods

Reagents. Analytical grade pyridine, chloral hydrate, olive oil and L-2-chlorophenylalanine were purchased from Shanghai Hengbai Biotech Co., Ltd., (Shanghai, China). Carbon tetrachloride (CCl_4) was purchased from Xilong Chemical Co., Ltd., (Guangdong, China) and bis- (trimethylsilyl) trifluoroacetamide (BSTFA) was purchased from Regis Technologies, Inc. (Morton Grove, IL, USA).

Animal Experiments. A total of 10, male Sprague-Dawley rats weighing 180-220 g and 7 weeks old were purchased from Anhui Medical University (Anhui, China). All the rats were allowed *ad libitum* access to food and water and housed individually in a facility at 18-22˚C, 40-60% humidity and a 12 h light-dark cycle. Surgery was performed under anesthesia with sodium pentobarbital (2 ml/kg, intraperitoneal injection, IP) purchased from Shanghai chemical reagent Co., Ltd. (Shanghai, China), and all efforts were made to minimize suffering. The protocol was approved by the Committee on the Ethics of Animal Experiments, Anhui University of Chinese Medicine (approval no. 2012AH-038-01; Anhui, China).

CCl_4 induction and treatment groups. Following 1 week of acclimatization, rats were randomly separated into two groups: Control group (n=5) and model group (n=5). The model group was treated with CCl_4 (0.1 ml/100 g 50% CCl_4, diluted to 50% in olive oil), injected subcutaneously into the back twice a week for 12 weeks to induce liver fibrosis. Samples of overnight (12 h) urine and serum were collected in metabolism cages from all rats 12 weeks following initial CCl_4 injection. All urine and serum samples were stored at -80˚C.

Histopathology. At the end of the experimental period, the animals were anesthetized with sodium pentobarbital (2 ml/kg, IP). A lobe of liver tissue (~2.0x2.0x0.3 cm) from each rat was removed during surgery and fixed in 10% neutral formalin at 25˚C (6-12 h), which prior to staining with hematoxylin and eosin (H&E) and Masson stains for histological examination as standard.

Sample preparation for GC/MS analysis. For samples of serum and urine, 100 μl of each was used. The urine sample was mixed with 10 μl urease suspension (160 mg/ml in water) in 1.5 ml EP tubes and vortexed for 10 sec. This was incubated at 37˚C for 1 h in order to decompose and remove excess urea. Serum and urine samples were then each mixed with 0.35 ml extraction liquid (3:1, Vmethanol:Vchloroform) and 50 μl L-2-chlorophenylalanine (0.2 mg/ml stock in H_2O) as an internal standard, in 1.5 ml EP tubes prior to 10 sec vortexing. The serum sample underwent centrifugation for 10 min at 23,500 x g at 4˚C. For samples of serum and urine, 0.35 ml supernatant was transferred into fresh 2 ml GC/MS glass vials, dried in a vacuum concentrator without heating. Methoxyamination reagent (Shanghai chemical reagent Co.,

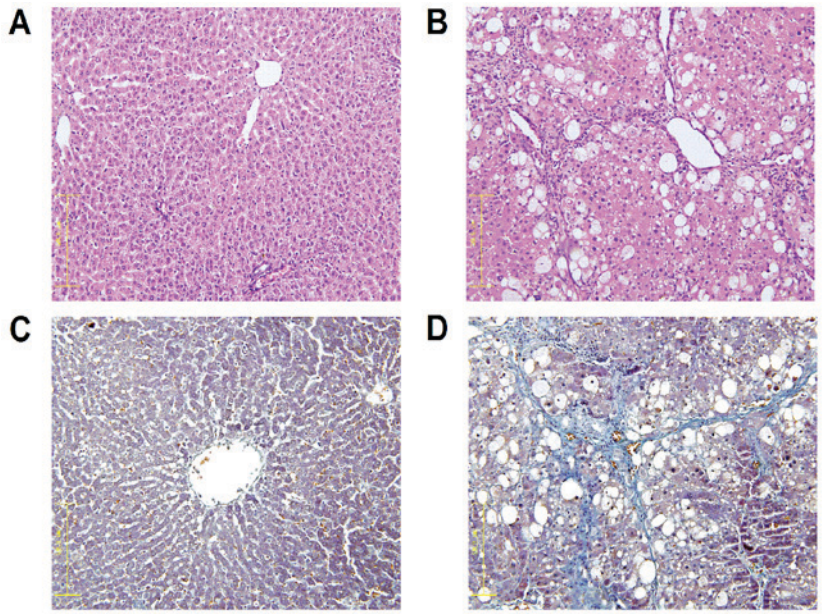

Figure 1. Histological examination of CCl_4-liver fibrosis in rats at 12 weeks (magnification, x200). Staining with H&E of the (A) control group and (B) model group. Staining with Masson stain of the (C) control group and (D) model group. CCl_4, carbon tetrachloride; H&E, hematoxylin and eosin stain.

Ltd.; 80 ml of 20 mg/ml in pyridine) was added and the samples underwent shaking for 2 h at 37˚C. A further 1 h of shaking at 70˚C was completed following the addition of 0.1 ml BSTFA regent (1% TriMethyl Chloro Silane, Tri Methyl Chloro Silane, v/v) to the sample aliquots. GC/MS analysis was completed when samples had cooled to room temperature.

An Agilent 7890a gas chromatograph system (Agilent Technologies, Santa Clara, CA, USA) coupled with a Pegasus 4D time-of-flight mass spectrometer (LECO Corporation®, Saint Joseph, MI, USA) was used to perform GC/MS analysis. This system utilizes a DB-5MS capillary column coated with 5% diphenyl cross-linked with 95% dimethylpolysiloxane (30x250 μm inner diameter, 0.25 μm film thickness; J&W Scientific, Agilent Technologies). The carrier gas used was helium, the gas flow rate through the column was 1 ml/min and the front inlet purge flow was 3 ml/min. A 1 μl aliquot of the analyte was injected in split-less mode. The initial temperature was kept at 80˚C for 12 sec, prior to being increased to 180˚C at a rate of serum: 10˚C/min for serum (urine: 5˚C/min), then to: 240˚C (urine: 220˚C) at a rate of: 5˚C/min (urine: 4˚C/min) and finally to: 290˚C (urine: 285˚C) at a rate of 20˚C/min for 11 min (urine: 10 min). The transfer line, injection and ion source temperatures were 270, 280, and 220˚C, respectively. The energy was -70 eV in electron impact mode. Full-scan mode was used to acquire mass spectrometry data, with an m/z range of 20-600 at a rate of 100 spectra/sec following a solvent delay of 492 sec.

Data analysis. Chroma TOF4.3X software (LECO corporation®) and LECO-Fiehn Rtx5 database were used to examine raw peaks (http://fiehnlab.ucdavis.edu/projects/FiehnLib/). The data baselines filtered and calibrated the peak alignment, deconvolution analysis, peak identification and integration of the peak area. The peaks were normalized to the total sum of the spectrum prior to multivariate analyses and the resulting data were analyzed using PCA and OPLS with SIMCA-P, software version 11.5 (Umetrics, Umeå, Sweden) following a unit variance procedure. The concentrations of potential biomarkers were represented as their relative areas (divided by the internal standard areas).

Statistical analysis. Quantitative data was presented as mean ± standard deviation. Statistical analysis was completed by one-way analysis of variance with Student Newman-Keuls test using the Statistic Package for Social Science software, version 17.0 (SPSS, Inc., Chicago, IL, USA). The histological grade of the liver was evaluated using Ridit analysis. $P<0.05$ was considered to represent a statistically significant difference.

Results

Histopathological changes to hepatic tissues. Fig. 1 presents liver tissue samples from each group following H&E and Masson staining. The control liver cell structure was clear with a large and round nucleus and abundant in cytoplasm with very little collagen deposition (Fig. 1A). The liver tissue samples from the model group exhibited greater hyperplasia of fibrous connective tissue, fatty degeneration, steatosis, cell necrosis, infiltration of inflammatory cells and a larger number of collagen fibers compared with the control group (Fig. 1B). Collagen fibers were stained blue following Masson staining. The portal area and interlobular septa had a small amount of collagen fibers deposited, which were shallow and small in the control group (Fig. 1C). However, the model group exhibited an increased amount of collagen fiber hyperplasia, a diffusing distribution of depth and a bulky and a false flocculus of hepatic lobule a divided hepatic lobule into the pseudolobule (Fig. 1D).

GC/MS spectra of the two groups. The typical GC/MS total ion current (TIC) chromatograms of rat serum and urine 12 weeks

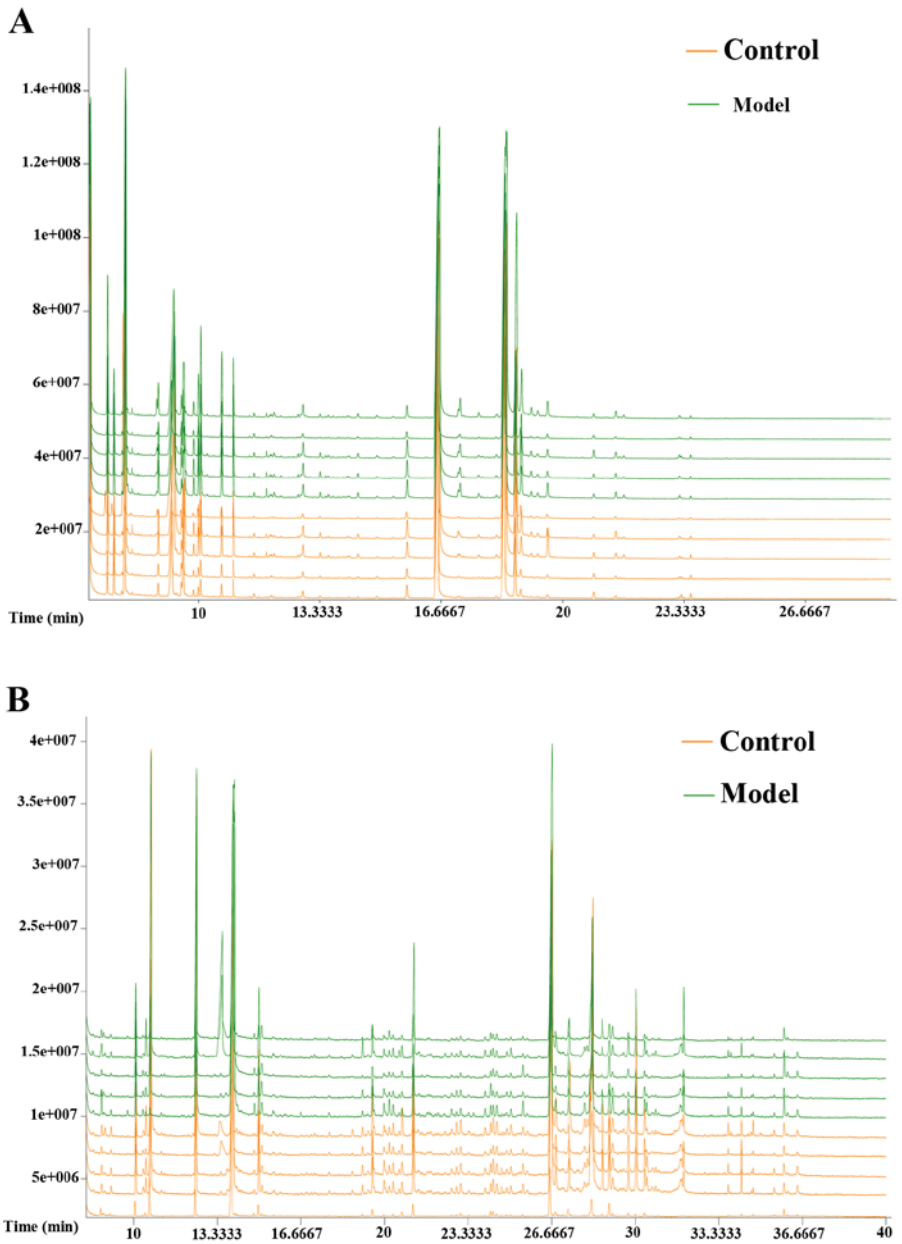

Figure 2. Typical GC/MS TIC chromatograms of CCl_4-liver fibrosis in rat serum and urine samples obtained from the two groups (control and model group) at 12 weeks. (A) Representative examples of serum results and (B) urine results. Samples obtained from different groups are illustrated at the top right corner of the figure with the control and model groups indicated the orange and green respectively. GC/MS, gas chromatography-mass spectrometry; TIC, total ion current; CCl_4, carbon tetrachloride.

following injection for the model group is presented in Fig. 2. The horizontal axis represents the time at which metabolites occur while the vertical axis represents the metabolite abundance. The peaks were considered to be representative chemical fingerprints of endogenous metabolites and the time above them represents their retention time (18). The area under a peak represents the relative richness of the metabolites. There were clear differences between the TIC profiles of the control and model groups. Spectra were pre-treated further and a pattern recognition analysis was performed to illuminate changes in the metabolic profiles.

PCA analysis. To understand the general trends and identify differences and outliers among the groups in serum and urine by GC/MS spectra, an unsupervised PCA was carried out to analyze the multivariate data (19,20). In the score plot of PCA, each data point represents the samples at week 12; the distance between points in the score plot indicates the similarity between samples. The results demonstrated that there were unsatisfactory separations in the score plots between the two groups (Fig. 3).

OPLS-analysis. To obtain a higher level of group separation and enhance recognition of variables contribution to classification, OPLS analysis was completed (21). The experimental results demonstrated that following OPLS analysis, the model group had been separated from the control group in serum and urine. This indicates that the model of liver fibrosis was produced successfully and endogenous metabolites in serum and urine of model rats were different compared with the control group (Fig. 4).

Identification of endogenous metabolites. To further investigate the targeting biomarkers on the metabolite profiles of liver fibrosis, the first principal component of variable importance projection (VIP) was obtained by assessing the influence of every term in the matrix variable X on all the variable Y's, where X and Y indicate the time and metabolite, respectively. VIP is normalized so that Sum $(VIP)^2$=K (number of terms in the matrix X.) VIP values >1.0 were selected as changed metabolites initially. The remaining variables were assessed by Student's t-test, which was reserved between two comparison groups. To further identify the potential biomarkers, commercial databases including the Kyoto Encyclopedia of Genes and Genomes (KEGG, accessible at: http://www.genome.jp/kegg/) and PubChem Compound (accessible at: https://pubchem.ncbi.nlm.nih.gov/) were utilized to search for metabolites (22). Based on the aforementioned analysis, seven metabolites in serum (Table I) and five metabolites in urine (Table II) were listed as significantly altered. For serum, the control group exhibited increased levels of carnitine, glucose and fucose, while isoleucine, L-malic acid, α-copper and hippuric acid levels were increased in the model group. In the urine, levels of N-acetyl-β-alanine and cytidine were increased in the control group compared with the model group while the model group had increased levels of 2-hydroxy butyric acid, isoleucine and corticoid.

Biological pathway and function analysis. Metabolite profiling analyzes a group of metabolites related to a specific metabolic pathway in biological states. To determine whether the observed changes in the metabolites reflected coordinate changes in defined metabolic pathways, CytoKEGG version 3.0.1 (Cytoscape Consortium, San Diego, CA, USA) was used for pathway construction. The pathways were based on seven metabolites in serum, including isoleucine, L-malic acid, α-copper, carnitine, hippuric acid, glutaric acid, glucose and fucose. The substances were associated with glucose, amino acid, P450, fatty acid or energy metabolism. CytoKEGG was also used for pathway construction based on the five altered metabolites in urine, including 2-hydroxy butyric acid, isoleucine, n-acetyl-β-alanine, cytidine and corticoid. The majority of these substances are related to amino acid metabolism, energy metabolism, glutathione biosynthesis and metabolism, nucleic acid metabolism or water-electrolyte metabolism (Fig. 5).

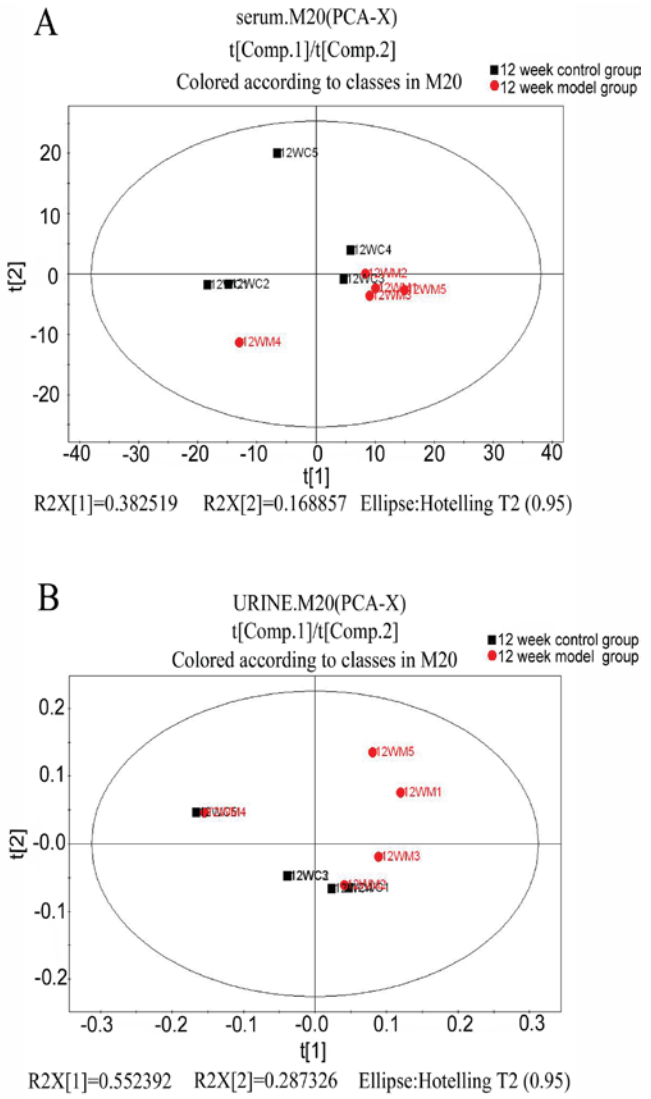

Figure 3. Principal component analysis score plot of CCl_4-liver fibrosis in rat (A) serum and (B) urine samples obtained from the two groups (control group in red, model group in black) at 12 weeks. Samples with different groups are indicated at the top right corner of the figure. CCl_4, carbon tetrachloride.

Discussion

Liver fibrosis is caused by a variety of factors, including hepatic stellate cell activation and proliferation leading to the synthesis and secretion of ECM. This leads to a large amount of collagen fiber deposition and eventually, the liver fibrosis (23). Liver fibrosis is the pathological basis of liver disease, which is a reversible lesion. However, the next step of liver disease, liver cirrhosis is irreversible (24). Therefore, it is important to develop methods to stop the progression of liver fibrosis.

CCl_4 is one of the chemicals known to be a common cause of acute chemical liver injury (25). As it causes a high incidence of ECM secretion, this model is easy to reproduce and is one of the common classical models of liver injury. The present study demonstrated that the hepatic cell swelling and marked necrosis observed in a number of collagen fibers in the model group may be induced by CCl_4, proving that it is a successful model of liver fibrosis.

Metabonomics is a novel analytical method that includes analysis of endogenous metabolites in various biofluids and tissues and indicates potential associations between metabolic profile changes and the physiological condition of the biosystems (26,27). Regarding the analysis of serum and urine samples at 12 weeks by GC/MS, the results indicated that CCl_4 exposure caused significant metabolic alterations in serum and urine samples, which affected related metabolic pathways.

Carnitine is an unusual amino acid synthesized by lysine and methionine in the liver. Carnitine has more important functions than other amino acids as it is involved in the process of protein synthesis and supplies energy through transporting fat into the mitochondria. Therefore, it is an indispensable factor in the process of fatty acid metabolism (28). A previous study indicated that the content of carnitine in serum for the model group was lower than in the control group (29). Thus,

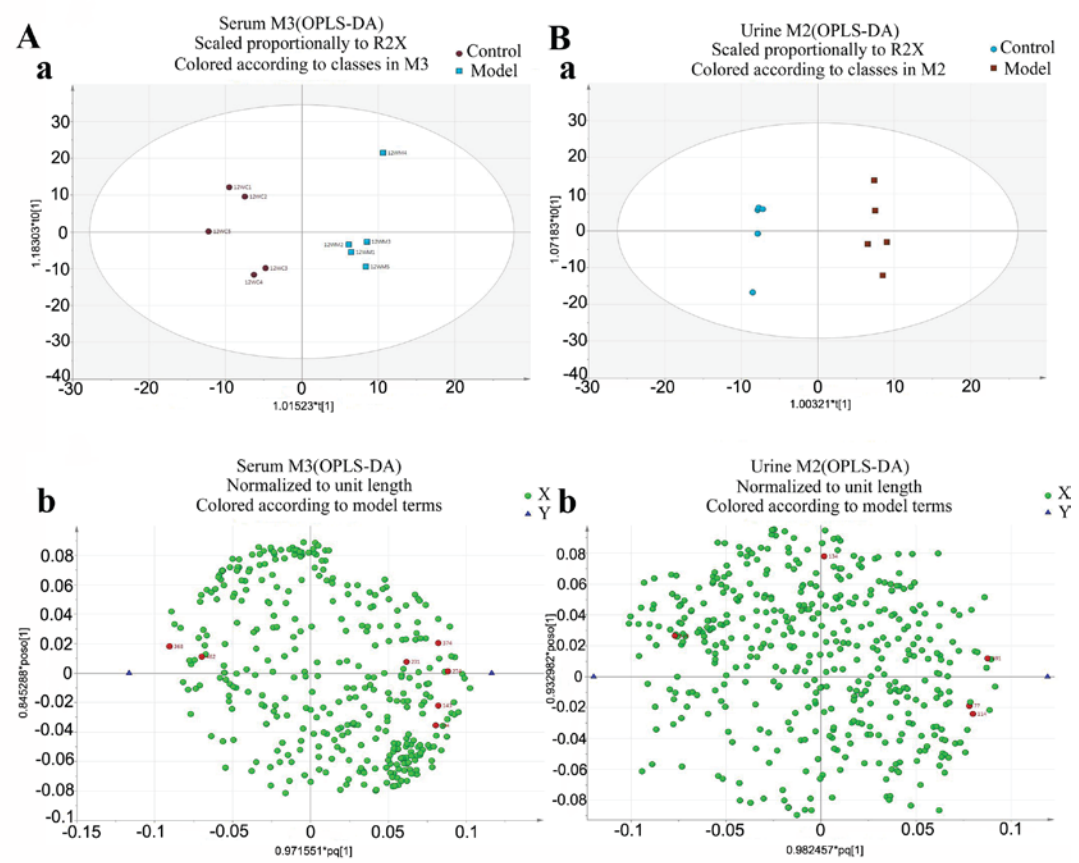

Figure 4. OPLS-DA score plot of CCl_4-liver fibrosis in rats serum and urine samples obtained from the two groups (control group, model group) at 12 weeks. Representative examples of (A) serum and (B) urine results. (Aa and Ba) These diagrams indicate that the model group had been separated from the control group. (Ab and Bb) Metabolic substances are represented as dots, red indicates the potential biomarkers. CCl_4, carbon tetrachloride; OPLS-DA; Orthogonal projections to latent structures-discriminant analysis.

the change of carnitine content in the model group affects the proceeding metabolism of fatty acids to a certain degree. The disorder of fatty acid metabolism may damage the mitochondria and lysosome, causing extracellular micro-organ damage and enhancing the toxicity of cytokines (30). This may lead to liver degeneration, inflammatory cell infiltration and consequently, fibrosis. Therefore, the present study indicates that there is an association between liver fibrosis and fatty acid metabolism.

In the serum, the content of glucose and fucose decreased in the model group compared with the control group. This indicates that liver diseases, such as liver fibrosis, are associated with a disturbance of carbohydrate metabolism. In the process of liver disease, the ability of insulin inactivation in the liver is inhibited and due to this, insulin levels in serum are markedly increased. This leads to the utilization of glucose, therefor enhancing the level of fucose while glucose levels decrease (31,32). This is consistent with the decrease of saccharides observed in the model group of rats in the current study. Saccharides, such as glucose, are the primary raw material for energy usage in the liver; they are also essential factors in the sugar metabolic pathways (33). In the present study, the content of glucose and fucose was downregulated in the serum of the model group, therefore, it is suggested that glucose and fucose levels are associated with glycometabolism changes. The change in glucose and fucose may also be related to the inactivation of insulin in the process of hepatic fibrosis (34).

In both serum and urine, the isoleucine was increased in the model group compared with the control group, indicating that an amino acid metabolism disorder may exist in liver fibrosis. A large number of experiments have demonstrated that hepatopathy is strongly linked to inflammatory and oxidative stress (35,36). Under oxidative stress, glycolysis and gluconeogenesis are inhibited. Isoleucine is a branched-chain amino acid, which is involved in the synthesis of glucose into triglycerides (TCA) in mammals by acetyl-coenzyme A (acetyl CoA) (37). If gluconeogenesis is restrained, it may lead to an increase of isoleucine in hepatic cells (38). As the important intermediate products of TCA, malic acid and α-copper glutaric acid are an energy supply for the body. Following CCl_4 injections in rats, CCl_4 decomposes into $CCl_3\cdot$ and CCl_3O_3, free radicals that induce oxidative stress by attacking the liver cells (39). It has been demonstrated that the TCA cycle is inhibited to reduce the generation of oxygen free radicals under oxidative stress and may be associated with liver diseases (40). Thus, an increase in the content of malic acid and α-copper glutaric acid may be caused by disturbance of the TCA cycle in the model group.

Alanine is an essential amino acid, transformed to pyruvic acid in hepatocytes and then pyruvic acid prior to entering the mitochondrial TCA pathway (41). N-acetyl-β-alanine is an alanine derivative, which can be converted into acetyl-CoA; this enters the mitochondrial pathway and participates in

Table I. Biomarkers and the changing trend of CCl_4-liver fibrosis in rat serum at 12 weeks.

Metabolite No.	Var ID (Primary)	Possible compounds	RT, min	VIP	Biomarker content in MG
1	143	isoleucine	9.86869	1.78195	Increase[a]
2	231	malic acid	12.2710	1.53429	Increase[b]
3	274	α-copper glutaric acid	13.4922	1.97915	Increase[a]
4	304	carnitine	14.3948	1.86529	Decrease[a]
5	368	glucose	17.5476	1.58140	Decrease[b]
6	374	hippuric acid	17.7654	1.78514	Increase[a]
7	462	fucose	26.9799	1.48060	Decrease[b]

519 peaks of the GC/MS spectra of the model and control groups were screened, corresponding to the number of the substance in serum when the VarID was imported into the software, VIP values >1.0 were selected as changed metabolites. From this, 7 metabolites from serum were demonstrated to be significantly altered. [a]P<0.01, [b]P<0.05 vs. control group. CCl_4, carbon tetrachloride; RT, retention time of the substance; VIP, variable importance projection; MG, model group.

Table II. Biomarkers and the changing trend of CCl_4-liver fibrosis in rat urine at 12 weeks.

Metabolite No.	Var ID (Primary)	Possible compounds	RT, min	VIP	Biomarker content in MG
1	77	2-hydroxy butyric acid	12.9871	2.48859	Increase[a]
2	114	isoleucine	15.0919	1.29507	Increase[a]
3	134	N-acetyl-β-alanine	16.9516	2.53192	Decrease[a]
4	314	cytidine	24.8217	2.38341	Decrease[a]
5	491	corticoid	34.8550	2.96963	Increase[a]

519 peaks of the GC/MS spectra of the model and control groups were screened, corresponding to the number of the substance in serum when the VarID was imported into the software, VIP values >1.0 were selected as changed metabolites. From this, 5 metabolites in the urine were demonstrated to be significantly altered. CCl_4, carbon tetrachloride; RT, retention time of the substance; VIP, variable importance projection; MG, model group. [a]P<0.05 vs. control group.

the TCA cycle, which is involved in energy metabolism and energy supply to the body (42). The variation of alanine and N-acetyl-β-alanine may be ascribed to the dysfunction of TCA. Through the analysis of urine metabolite spectrum in rats, it was demonstrated that the content of N-acetyl-β-alanine was reduced in the model rats, which may be associated with disturbance of energy metabolism.

Compared with the control group, there was an increase of hippuric acid in the model group. Hippuric acid is produced by combining glycine with benzoic acid during cytochrome P450 catalysis (43). Consequently, changes in hippuric acid content in the model group may occur following changes in cytochrome P450, which is closely related to the formation of liver fibrosis.

The content of 2-hydroxy butyric acid in the model group is increased compared with in the control group. 2-hydroxy butyric acid is a type of organic acid derived from α-butanone acid and is involved in the synthesis and metabolism of glutathione (44). Changes in glutathione synthesis consequently result in the content of 2-hydroxy butyric acid. It has been demonstrated that glutathione can protect the liver from oxidative stress damage, which is closely associated with liver disease (45).

Cytosine is one of the pyrimidine bases in nucleic acids and participates in complementary base pairing, which forms cytidine, synthesizes cytidylic acid at a nucleoside triphosphate level and participates in nucleic acid synthesis and metabolism (46). The liver is the area of nucleoside synthesis within the body. Therefore, consistent with the results of the present study, a number of reasons including injury, inflammation and fibrosis lead to the loss of liver function and nucleic acid synthesis insufficiency. In urine, the content of cytidine in the model group is lower than in the control group, which may relate to a disturbance of nucleic acid metabolism.

The content of corticoid in the model group was increased compared with the control group. Corticoid includes glucocorticoid and mineralocorticoid, while aldosterone is a primary mineralocorticoid that is primarily regulated by the renin-angiotensin-aldosterone system (RAAS), sodium and potassium in the blood, which in turn is regulated by water-electrolyte metabolism (47). It has been indicated that RAAS locally exists in the liver (48). When hepatic fibrosis occurs, the level of inactivated aldosterone decreases depending on how much the liver function subsides, thus RAAS emerges at a high activity and is closely associated

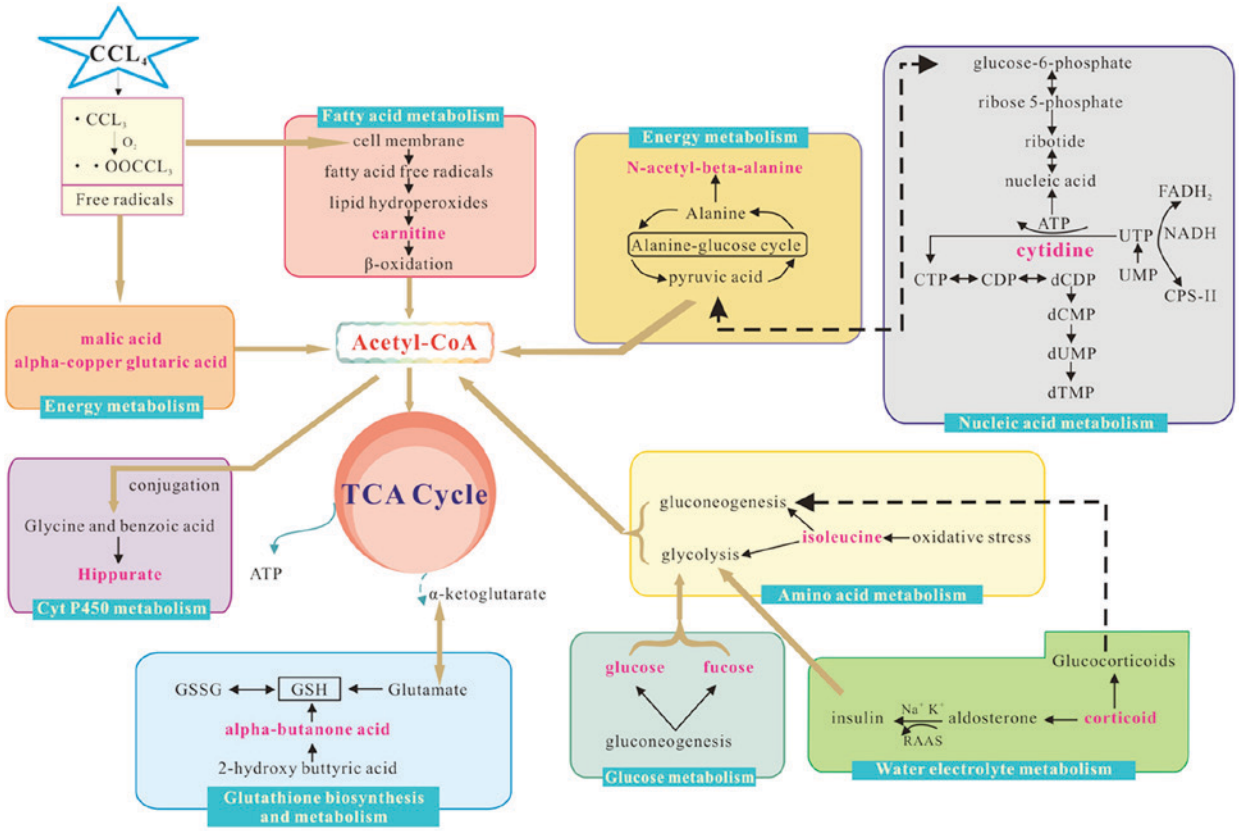

Figure 5. Interference of the metabolic pathway analysis in the control and model groups. Red text denotes the endogenous metabolites used to explain the possible metabolic pathways, and box plot of endogenous metabolites next to its metabolic pathways. CCl_4, carbon tetrachloride; Acetyl-CoA, Acetyl coenzyme A; RAAS, Renin-Angiotensin-Aldosterone System; ATP, adenosine triphosphate; CTP, Cytidine triphosphate; CDP, Cytidine diphosphate; dCDP, deoxygenation cytidine diphosphate; dCMP, deoxygenation adenosine monophosphate; dUMP, deoxygenation uridine monophosphate; UTP, uridine triphosphate; UMP, uridine monophosphate; $FADH_2$, flavine adenine dinucleotide 2; NADH, reduced form of nicotinamide-adenine dinucleotid; Cps-II, carbamyl phosphate synthetase-II; GSSG: oxidized glutathione; GSH: glutathione; TCA: tricarboxylic acid cycle.

with the formation of liver fibrosis. Therefore, the change of corticoid content in the model group may be a reaction to the change in water-electrolyte metabolism.

In conclusion, the present study demonstrated that exposure to CCl_4 induced liver damage and significantly altered a number of metabolic pathways. Histological results indicated that the model of liver fibrosis induced by CCl_4 in rats was successful. Pattern recognition with multivariate statistical analysis indicated that the metabolic profile of CCl_4-induced liver fibrosis was clearly separated from the control group. Potential biomarkers were identified, seven metabolites in serum and five metabolites in urine, which may be associated with the disturbance of energy, amino acid, carbohydrate, cytochrome P450, glutathione synthesis, fatty acid, nucleic acid and water-electrolyte metabolisms. The current study provided novel drug targets and demonstrated that metabonomic methods based on GC/MS maybe a useful tool for determining the pathogenesis of diseases.

Acknowledgements

The present study was financially supported by National Natural Science Foundation of China (grant no. 81102874). We are grateful to Ms. Jie Xu and Dr Junliang Deng (Biotree Bio-technology Co., Ltd., Shanghai, China) for providing help with data analysis.

References

1. Zira A, Kostidis S, Theocharis S, Sigala F, Engelsen SB, Andreadou I and Mikros E: 1H NMR-based metabonomics approach in a rat model of acute liver injury and regeneration induced by CCl_4 administration. Toxicology 303: 115-124, 2013.
2. Zheng J, Wu C, Lin Z, Guo Y, Shi L, Dong P, Lu Z, Gao S, Liao Y, Chen B and Yu F: Curcumin up-regulates phosphatase and tensin homologue deleted on chromosome 10 through microRNA-mediated control of DNA methylation-a novel mechanism suppressing liver fibrosis. FEBS J 281: 88-103, 2014.
3. Zhang S, Wu J, Wang H, Wang T, Jin L, Shu D, Shan W and Xiong S: Liposomal oxymatrine in hepatic fibrosis treatment: Formulation, in vitro and in vivo assessment. AAPS PharmSciTech 15: 620-629, 2014.
4. Sun LL, Chang W, Jiao LQ, Cui X and Dong G: Hepatic fibrosis and supersonic shear imaging in patients with different etiological chronic hepatic diseases. J Biol Regul Homeost Agents 30: 761-765, 2016.
5. Seo KW, Sohn SY, Bhang DH, Nam MJ, Lee HW and Youn HY: Therapeutic effects of hepatocyte growth factor-overexpressing human umbilical cord blood-derived mesenchymal stem cells on liver fibrosis in rats. Cell Biol Int 38: 106-116, 2014.
6. Lee JE, Lee JM, Lee KB, Yoon JH, Shin CI, Han JK and Choi BI: Noninvasive assessment of hepatic fibrosis in patients with chronic hepatitis B viral infection using magnetic resonance elastography. Korean J Radiol 15: 210-217, 2014.
7. Ozkurt H, Keskiner F, Karatag O, Alkim C, Erturk SM and Basak M: Diffusion weighted MRI for hepatic fibrosis: Impact of b-Value. Iran J Radiol 11: e3555, 2014.
8. Lu Q, Luo Y, Yuan CX, Yan LN, Wu H and Zhang ZW: Ultrasound imaging of bridge vessel transplant used to reconstruct the tributary of middle hepatic vein in living donor liver transplantation. Sichuan Da Xue Xue Bao Yi Xue Ban 38: 529-531, 2007 (In Chinese).

9. Duan J, Hu C, Luo S, Zhao X and Wang T: Microcomputed tomography with diffraction-enhanced imaging for morphologic characterization and quantitative evaluation of microvessel of hepatic fibrosis in rats. PLoS One 8: e78176, 2013.
10. Razek AA, Khashaba M, Abdalla A, Bayomy M and Barakat T: Apparent diffusion coefficient value of hepatic fibrosis and inflammation in children with chronic hepatitis. Radiol Med 119: 903-909, 2014.
11. Leeming DJ, Byrjalsen I, Jiménez W, Christiansen C and Karsdal MA: Protein fingerprinting of the extracellular matrix remodelling in a rat model of liver fibrosis-a serological evaluation. Liver Int 33: 439-447, 2013.
12. Manna SK, Thompson MD and Gonzalez FJ: Application of mass spectrometry-based metabolomics in identification of early noninvasive biomarkers of alcohol-induced liver disease using mouse model. Adv Exp Med Biol 815: 217-238, 2015.
13. Huang X, Shao L, Gong Y, Mao Y, Liu C, Qu H and Cheng Y: A metabonomic characterization of CCl_4-induced acute liver failure using partial least square regression based on the GC/MS metabolic profiles of plasma in mice. J Chromatogr B Analyt Technol Biomed Life Sci 870: 178-185, 2008.
14. Gou X, Tao Q, Feng Q, Peng J, Zhao Y, Dai J, Wang W, Zhang Y, Hu Y and Liu P: Urine metabolic profile changes of CCl_4-liver fibrosis in rats and intervention effects of Yi Guan Jian Decoction using metabonomic approach. BMC Complement Altern Med 13: 123, 2013.
15. Ressom HW, Xiao JF, Tuli L, Varghese RS, Zhou B, Tsai TH, Ranjbar MR, Zhao Y, Wang J, Di Poto C, *et al*: Utilization of metabolomics to identify serum biomarkers for hepatocellular carcinoma in patients with liver cirrhosis. Anal Chim Acta 743: 90-100, 2012.
16. Wu H, Liu T, Ma C, Xue R, Deng C, Zeng H and Shen X: GC/MS-based metabolomic approach to validate the role of urinary sarcosine and target biomarkers for human prostate cancer by microwave-assisted derivatization. Anal Bioanal Chem 401: 635-646, 2011.
17. Sun S, Dai J, Fang J, Gou X, Cao H, Zheng N, Wang Y, Zhang W, Zhang Y, Jia W and Hu Y: Differences of excess and deficiency zheng in patients with chronic hepatitis B by urinary metabonomics. Evid Based Complement Alternat Med 2013: 738245, 2013.
18. Feng B, Wu S, Liu F, Gao Y, Dong F and Wei L: Metabonomic analysis of liver tissue from BALB/c mice with D-galactosamine/lipopolysaccharide-induced acute hepatic failure. BMC Gastroenterol 13: 73, 2013.
19. Yu K, Sheng G, Sheng J, Chen Y, Xu W, Liu X, Cao H, Qu H, Cheng Y and Li L: A metabonomic investigation on the biochemical perturbation in liver failure patients caused by hepatitis B virus. J Proteome Res 6: 2413-2419, 2007.
20. Lin B, Zhang H, Lin Z, Fang Y, Tian L, Yang H, Yan J, Liu H, Zhang W and Xi Z: Studies of single-walled carbon nanotubes-induced hepatotoxicity by NMR-based metabonomics of rat blood plasma and liver extracts. Nanoscale Res Lett 8: 236, 2013.
21. Chen J, Wang W, Lv S, Yin P, Zhao X, Lu X, Zhang F and Xu G: Metabonomics study of liver cancer based on ultra performance liquid chromatography coupled to mass spectrometry with HILIC and RPLC separations. Anal Chim Acta 650: 3-9, 2009.
22. Ma J, Yu J, Su X, Zhu C, Yang X, Sun H, Chen D, Wang Y, Cao H and Lu J: UPLC-MS-based serum metabonomics for identifying acute liver injury biomarkers in Chinese miniature pigs. Toxicol Lett 225: 358-366, 2014.
23. Chen B, Ye B, Zhang J, Ying L and Chen Y: RDW to platelet ratio: A novel noninvasive index for predicting hepatic fibrosis and cirrhosis in chronic hepatitis B. PLoS One 8: e68780, 2013.
24. Frias M, Rodriguez-Cano D, Cuenca-López F, Macías J, Gordon A, Manzanares-Martín B, Pineda JA, Camacho Á, Torre-Cisneros J, Peña J, *et al*: HLA-B18 as risk factor of liver fibrosis progression in HIV/HCV treatment-experienced patients. Pharmacogenomics J: Oct 25, 2016 (Epub ahead of print)].
25. Chheda TK, Shivakumar P, Sadasivan SK, Chanderasekharan H, Moolemath Y, Oommen AM, Madanahalli JR and Marikunte VV: Fast food diet with CCl_4 micro-dose induced hepatic-fibrosis-a novel animal model. BMC Gastroenterol 14: 89, 2014.
26. Gou X, Tao Q, Feng Q, Peng J, Sun S, Cao H, Zheng N, Zhang Y, Hu Y and Liu P: Urinary metabonomics characterization of liver fibrosis induced by CCl_4 in rats and intervention effects of Xia Yu Xue Decoction. J Pharm Biomed Anal 74: 62-65, 2013.
27. Sun H, Zhang AH, Zou DX, Sun WJ, Wu XH and Wang XJ: Metabolomics coupled with pattern recognition and pathway analysis on potential biomarkers in liver injury and hepatoprotective effects of yinchenhao. Appl Biochem Biotechnol 173: 857-869, 2014.
28. Giudetti AM, Stanca E, Siculella L, Gnoni GV and Damiano F: Nutritional and hormonal regulation of citrate and carnitine/acyl-carnitine transporters: Two mitochondrial carriers involved in fatty acid metabolism. Int J Mol Sci 17: pii: E817, 2016.
29. Demiroren K, Dogan Y, Kocamaz H, Ozercan IH, Ilhan S, Ustundag B and Bahcecioglu IH: Protective effects of L-carnitine, N-acetylcysteine and genistein in an experimental model of liver fibrosis. Clin Res Hepatol Gastroenterol 38: 63-72, 2014.
30. Muroya Y, Ito O, Rong R, Takashima K, Ito D, Cao P, Nakamura Y, Joh K and Kohzuki M: Disorder of fatty acid metabolism in the kidney of PAN-induced nephrotic rats. Am J Physiol Renal Physiol 303: F1070-F1079, 2012.
31. Manco M and Nobili V: Beta-cell glucose sensitivity in patients with liver fibrosis. Gut 57: 1023, 2008.
32. Haukeland JW, Konopski Z, Linnestad P, Azimy S, Marit Løberg E, Haaland T, Birkeland K and Bjøro K: Abnormal glucose tolerance is a predictor of steatohepatitis and fibrosis in patients with non-alcoholic fatty liver disease. Scand J Gastroenterol 40: 1469-1477, 2005.
33. Zant R, Melter M, Beck D, Ameres M, Knoppke B and Kunkel J: Glucose metabolism and associated outcome after pediatric liver transplantation. Transplant Proc 48: 2709-2713, 2016.
34. Haraguchi M, Miyaaki H, Ichikawa T, Shibata H, Honda T, Ozawa E, Miuma S, Taura N, Takeshima F and Nakao K: Glucose fluctuations reduce quality of sleep and of life in patients with liver cirrhosis. Hepatol Int 11: 125-131, 2017.
35. Bala S, Csak T, Saha B, Zatsiorsky J, Kodys K, Catalano D, Satishchandran A and Szabo G: The pro-inflammatory effects of miR-155 promote liver fibrosis and alcohol-induced steatohepatitis. J Hepatol 64: 1378-1387, 2016.
36. Araújo Júnior RF, Garcia VB, Leitão RF, Brito GA, Miguel Ede C, Guedes PM and de Araújo A: Carvedilol improves inflammatory response, oxidative stress and fibrosis in the alcohol-induced liver injury in rats by regulating kuppfer cells and hepatic stellate cells. PLoS One 11: e0148868, 2016.
37. Wang H, Zhang Y, Wang T, You H and Jia J: N-methyl-4-isoleucine cyclosporine attenuates CCl -induced liver fibrosis in rats by interacting with cyclophilin B and D. J Gastroenterol Hepatol 26: 558-567, 2011.
38. Tajiri K and Shimizu Y: Branched-chain amino acids in liver diseases. World J Gastroenterol 19: 7620-7629, 2013.
39. Britton RS and Bacon BR: Role of free radicals in liver diseases and hepatic fibrosis. Hepatogastroenterology 41: 343-348, 1994.
40. Miyake M, Innami T and Kakimoto Y: A beta-citryl-L-glutamate-hydrolysing enzyme in rat testes. Biochim Biophys Acta 760: 206-214, 1983.
41. Kadotani A, Fujimura M, Nakamura T, Ohyama S, Harada N, Maruki H, Tamai Y, Kanatani A and Eiki J: Metabolic impact of overexpression of liver glycogen synthase with serine-to-alanine substitutions in rat primary hepatocytes. Arch Biochem Biophys 466: 283-289, 2007.
42. Burelle Y, Fillipi C, Péronnet F and Leverve X: Mechanisms of increased gluconeogenesis from alanine in rat isolated hepatocytes after endurance training. Am J Physiol Endocrinol Metab 278: E35-E42, 2000.
43. Volpe DA, Tobin GA, Tavakkoli F, Dowling TC, Light PD and Parker RJ: Effect of uremic serum and uremic toxins on drug metabolism in human microsomes. Regul Toxicol Pharmacol 68: 297-303, 2014.
44. Bouthillier LP, Pushpathadam JJ and Binette Y: Study of the metabolism of 2-hydroxy-4-amino-butyric acid, a product of gamma-hydroxyglutamic acid decarboxylation. Can J Biochem 44: 171-177, 1966.
45. Gallagher EP, Gardner JL and Barber DS: Several glutathione S-transferase isozymes that protect against oxidative injury are expressed in human liver mitochondria. Biochem Pharmacol 71: 1619-1628, 2006.
46. Cai J, Gong R, Yan F, Yu C, Liu L, Wang W, Lin Y, Guo M, Li W and Huang Z: ZNF300 knockdown inhibits forced megakaryocytic differentiation by phorbol and erythrocytic differentiation by arabinofuranosyl cytidine in K562 cells. PLoS One 9: e114768, 2014.
47. Masoumi A, Ortiz F, Radhakrishnan J, Schrier RW and Colombo PC: Mineralocorticoid receptor antagonists as diuretics: Can congestive heart failure learn from liver failure? Heart Fail Rev 20: 283-290, 2015.
48. Queisser N, Happ K, Link S, Jahn D, Zimnol A, Geier A and Schupp N: Aldosterone induces fibrosis, oxidative stress and DNA damage in livers of male rats independent of blood pressure changes. Toxicol Appl Pharmacol 280: 399-407, 2014.